In situ control of the catalyst efficiency in chemical vapor deposition of vertically aligned carbon nanotubes on predeposited metal catalyst films

Gyula Eres,[a] A. A. Puretzky, D. B. Geohegan, and H. Cui
Condensed Matter Sciences Division, Oak Ridge National Laboratory, Oak Ridge, Tennessee 37831

(Received 10 November 2003; accepted 19 January 2004)

Premature termination of growth, presumably because of catalyst deactivation, is an undesirable side effect of chemical vapor deposition of vertically aligned carbon nanotubes on predeposited metal catalyst films. The addition of ferrocene, an effective precursor for *in situ* Fe formation, was found to enhance carbon nanotube growth rates and extend growth to 3.25 mm thick carbon nanotube films. Ferrocene was introduced into the gas stream by thermal evaporation concurrently with acetylene using a specially constructed source. The key factor facilitating the growth of thick carbon nanotube films was the independent and precise control of the ferrocene amount in the feedstock. The carbon nanotube films were characterized by scanning and transmission electron microscopy, and Raman spectroscopy. The temperature dependence of the carbon nanotube growth with ferrocene exhibits a steep drop at high substrate temperatures and a loss of vertical alignment at 900 °C. The negative temperature coefficient of the growth rate suggests that the reaction mechanism of vertically aligned carbon nanotube growth is governed by a heterogeneous intermediate step. © *2004 American Institute of Physics.* [DOI: 10.1063/1.1668325]

Vertically aligned (VA) arrays of carbon nanotubes (CNTs) are attractive for a wide range of nanoelectronic device applications.[1] Thermal chemical vapor deposition (CVD),[2,3] and plasma enhanced CVD[4,5] are presently the only growth techniques capable of directly producing VA-CNTs on various substrates. The fact that metal film deposition is compatible with high resolution lithography techniques represents a distinct advantage of metal catalyst films over other methods of catalyst pattern formation in nanoelectronic device fabrication.[5–7]

The CNT characteristics and growth rates depend strongly on the composition and the thickness of the metal catalyst films.[8,9] In addition to the active catalyst, the predeposited metal films contain other metals that promote nucleation of CNTs and/or function as a diffusion barrier.[9] A trilayer consisting of Al, Fe, and Mo, reported by Delzeit was found to be the most effective predeposited film for patterned growth of VA-CNTs.[10] CNT growth on metal catalyst films exhibits a saturation effect observed previously in carbon filament growth and bulk carbon deposition on transition metals.[11,12] The catalyst deactivation that leads to CNT growth termination after a few hundred microns of growth is a major drawback of CNT CVD on metal catalyst films.[13,14] In this letter we demonstrate that the addition of ferrocene, $Fe(C_5H_5)_2$, a precursor for *in situ* Fe formation enhances the effectiveness of the predeposited catalyst films, and postpones the onset of CNT growth saturation resulting in higher CNT growth rates and thicker CNT films.

$Fe(C_5H_5)_2$ has been used extensively as a source of Fe catalyst in CNT growth.[15–17] $Fe(C_5H_5)_2$ is typically dissolved in a hydrocarbon solvent, such as xylene, or benzene, which serves as the carbon feedstock.[16] The CNT growth mechanism is thought to be initiated by decomposition of $Fe(C_5H_5)_2$ and formation of Fe nanoparticles.[15–17] The total CNT yield, the amount of Fe in the films, and the diameter distribution decrease with the concentration of $Fe(C_5H_5)_2$ in the solution.[16] Under these conditions the CNT diameters range from 10 to 100 nm, and the films contain a large number of encapsulated Fe nanoparticles in both the root and the tip region.[15,16] Therefore, precise dosing of $Fe(C_5H_5)_2$ could be used to control the CNT diameters and to reduce the amount of residual Fe in the CNT films.

The $Fe(C_5H_5)_2$ source illustrated in Fig. 1 consists of a Ta cartridge, which is 0.22 in. in diameter and 2 in. long. The open end of this cartridge is sealed with a stainless steel plug in which a 250 μm hole was drilled. The cartridge is heated by a 2 in. long, 0.25 in. inside diameter, pyrolytic boron nitride nozzle heater. The heater assembly is mounted on a KF40 flange that mates with the inlet flange of the reactor. The temperature of $Fe(C_5H_5)_2$ is measured by a thermocouple that is in thermal contact with the cartridge. The transfer of $Fe(C_5H_5)_2$ into the gas stream occurs by sublimation at temperatures slightly below the melting point of $Fe(C_5H_5)_2$ (174 °C). The cartridge is loaded with 200–300 mg of $Fe(C_5H_5)_2$. The exact amount of $Fe(C_5H_5)_2$ used in each experiment is determined by weighing the cartridge.

The multilayer metal catalyst films were deposited on 4 in. Si(100) wafers by electron beam evaporation at room

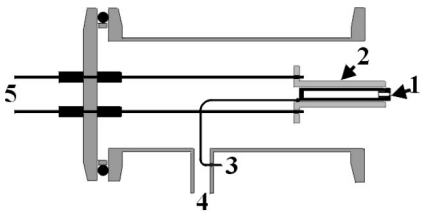

FIG. 1. Sketch of the ferrocene thermal evaporation source: (1) nozzle orifice, (2) pyrolytic boron nitride heater, (3) thermocouple, (4) gas inlet, and (5) power feedthrough.

[a]Electronic mail: eresg@ornl.gov

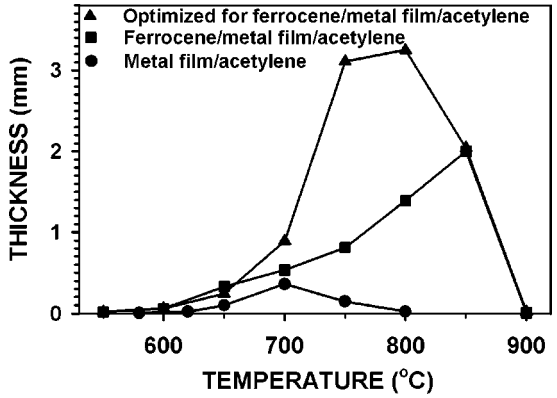

FIG. 2. Temperature dependence of the CNT film thickness. Solid dots correspond to CVD on the Al/Fe/Mo multilayer film using a 100 sccm/2.9 sccm hydrogen/acetylene ratio. Solid squares represent CVD growth with addition of 4 mg/h of ferrocene. Filled triangles represent CNT growth for optimized ratio of 4 mg/h of ferrocene to 12.4 sccm of acetylene.

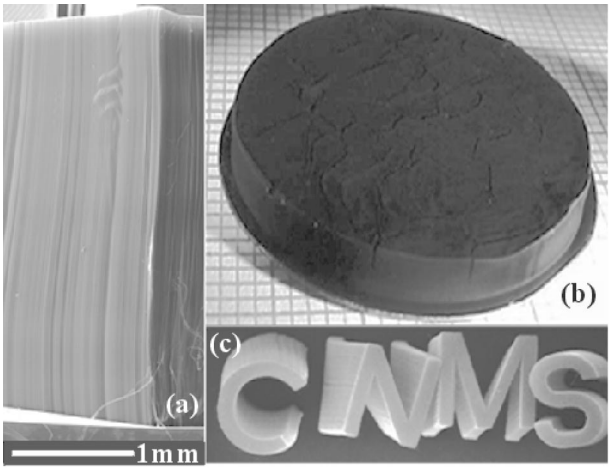

FIG. 3. (a) Low magnification SEM image of the 3.25 mm thick CNT film; (b) optical image of a 2.5 mm thick CNT film grown on a 1 in. diameter Si wafer, placed on mm division graph paper; (c) SEM image of the CNMS logo grown on a Si wafer, the letters are 1.5 mm tall and the linewidth is 10 μm. The catalyst pattern in (c) was produced by liftoff using a photolithographically defined resist pattern.

temperature. The films consisted of a stack of 10 nm of Al, 1 nm of Fe, and 0.2 nm of Mo.[10,14] To avoid inadvertent experiment-to-experiment variations in the catalyst film thickness and composition, all CNT films were grown on 10×25 mm^2 pieces that were cleaved from one wafer. CVD was performed slightly above atmospheric pressure in a single stage furnace equipped with a 1.5 in. diameter quartz tube. The growth temperature was in the range 550–900 °C. When the desired growth temperature was reached, the $Fe(C_5H_5)_2$ source was started in a flow of 500 sccm Ar and 100 sccm H_2. C_2H_2 was introduced a few minutes later when the $Fe(C_5H_5)_2$ source reached a temperature of about 150 °C. The flow rate of C_2H_2 was in the range from 2 to 12.4 sccm. In a typical growth run of 1 h at a source temperature around 150–170 °C, 2–5 mg of $Fe(C_5H_5)_2$ were used. The optimal growth selectivity for patterned growth was observed at a H_2 flow rate of 100 sccm. To avoid cross contamination by the reactor, the films with and without $Fe(C_5H_5)_2$ were grown in different quartz tubes. Additionally, the quartz tube used with $Fe(C_5H_5)_2$ was scraped clean after each run and heated to 800 °C in a low flow of atmospheric air to burn off residual reaction products from a previous run.

The samples were analyzed using SEM (Hitachi, S-4700) and TEM (Hitachi, HF-2000) imaging and Raman spectroscopy (Renishaw, System 1000). In Fig. 2, the film thickness as a function of the substrate temperature is shown for three different growth conditions. Each data point in these plots represents CNT growth for 1 h. The thickness of the films was determined from edge-on SEM images of cleaved samples using a special 90° sample holder. The solid dots represent growth conditions optimized for maximum CNT film thickness on a given predeposited metal catalyst film in terms of the C_2H_2/H_2 flow ratio (2.9 sccm/100 sccm). Inadvertent variations in the nominal composition of the catalyst films were found to produce large film-to-film fluctuations in the maximum CNT thickness. The data series represented by the solid squares shows the film thickness with addition of $Fe(C_5H_5)_2$ (4 mg/h) under the same gas flow conditions as in the first data set. Note the increase of the film thickness (growth rate) and the shift of the maximum of the growth curve toward higher temperatures. Further increase in the CNT growth rates shown by the solid triangles was achieved by optimizing the $Fe(C_5H_5)_2/C_2H_2$ ratio in the feedstock. With $Fe(C_5H_5)_2$ CNT growth was no longer dominated by the catalyst film composition. Instead, the growth rate and the film thickness strongly depended on the amount of $Fe(C_5H_5)_2$ in the feedstock. A maximum CNT length of 3.25 mm shown in Fig. 3(a) has been obtained for a 4 mg/h-to-12.4 sccm of the $Fe(C_5H_5)_2/C_2H_2$ ratio. There is no growth enhancement if the $Fe(C_5H_5)_2$ flow is shut off before starting the flow of C_2H_2. The full extent of the growth enhancement can be realized only with concurrent acetylene and ferrocene flow.

The TEM, SEM, and Raman data reveal no substantial difference in the structure and diameter distribution among the CNTs grown at different growth conditions. The temperature dependence of the CNT properties in each particular data set follows similar trends that were outlined previously for growth using the Al/Fe/Mo multilayered films.[14] Raman spectroscopy and TEM imaging show that the bulk of the CNT films consist of multiwall CNTs. The TEM images from the 3.25 mm thick film reveal a well developed wall structure with four to ten shells [see Fig. 4(d)] and a diameter distribution that peaks around 10 nm. A clear signal corresponding to a single wall (SW) breathing mode was observed in the Raman spectra when the films were scanned from the top. No SW signal was observed when long CNT bundles were scanned edge-on, suggesting that the SW CNTs are located on the top of the films,[16] and not intertwined in the films.[18] In contrast with the solvent injection CVD technique,[16] TEM and SEM images for optimal $Fe(C_5H_5)_2/C_2H_2$ ratio show a substantially reduced number of Fe particles in the root area that were enclosed in carbon or attached to the outside walls of the CNTs. No such particles were observed in the tip area of the CNT films [see Fig. 4(a)], nor along the length of the CNTs [see Fig. 4(b) and 4(c)].

A comparison of the growth curves in Fig. 2 suggests that the addition of $Fe(C_5H_5)_2$ fundamentally alters the growth mechanism of VA-CNTs. The small amount of

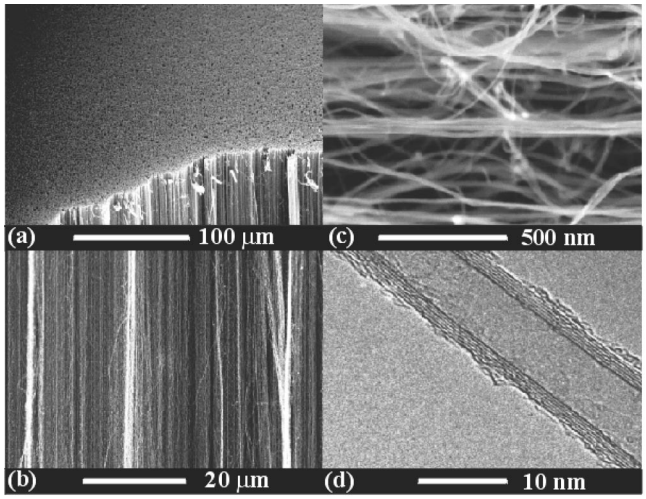

FIG. 4. (a) SEM image of the top of the CNT films; (b) SEM image of the side wall of the CNT films; (c) high resolution SEM image of CNT alignment in the films; (d) high resolution TEM image of a typical multiwall CNT.

$Fe(C_5H_5)_2$ corresponding to an equivalent continuous flow rate of 1.5×10^{-2} sccm, rules out the possibility that the growth enhancements are supply related. Rather, the reaction products resulting from localized decomposition of $Fe(C_5H_5)_2$ on the metal film (but not on Si)[19] act in a way that enhances the catalytic activity of the metal film toward CNT growth. Selective area growth of CNTs on patterned substrates shown in Figs. 3(b) and 3(c) clearly illustrates that the decomposition of $Fe(C_5H_5)_2$ is surface specific.

The mechanism by which $Fe(C_5H_5)_2$ promotes VA-CNT growth is not presently clear. The results of the ongoing study will be reported in the future. Here we present plausible mechanisms that agree with the experimental trends. The simplest mechanism by which $Fe(C_5H_5)_2$ decomposition can enhance the catalytic activity is by providing active Fe to shift the composition of the predeposited metal catalyst films. A more intriguing pathway by which $Fe(C_5H_5)_2$ could enhance CNT growth is by producing molecular intermediate decomposition products that actively mediate C_2H_2 dehydrogenation and incorporation into CNTs. The active Fe hypothesis is supported by the fact that CVD of $Fe(C_5H_5)_2$ in H_2 (with no C_2H_2) at and above 750 °C produces only a Fe film, but no CNTs. At 600 °C only an Fe-rich carbonaceous deposit was obtained. Note that the homogeneous gas-phase thermal decomposition threshold for $Fe(C_5H_5)_2$ is 850 °C, and that heterogeneous decomposition of $Fe(C_5H_5)_2$ occurs below this temperature.[20]

A particularly striking feature of the VA-CNT growth process is a steep drop in the film thickness at high temperatures. In a recent report, alloying of Fe with Si was suggested to reduce the catalytic activity of Fe resulting in lower CNT growth rates above 850 °C.[21] However, a similar decrease in CNT film thickness observed when using sapphire in a few high temperature growth experiments rules out silicide formation as the cause of the growth rate reduction. This negative temperature coefficient growth regime is not unique to VA-CNT growth. Similar behavior was observed in carbon filament growth[11] and bulk carbon deposition from hydrocarbons on transition metals.[22]

In conclusion, we report on $Fe(C_5H_5)_2$ induced enhancement of CNT growth by CVD resulting in 3.25 mm thick VA-CNT films. Comparison of the temperature dependent growth curves shows that the addition of $Fe(C_5H_5)_2$ fundamentally alters the growth mechanism of VA-CNTs on predeposited metal catalyst films that is manifested in a shift of the growth curves toward higher temperatures. A particularly striking feature of the growth curves is a steep drop of the film thickness at high substrate temperatures. The negative temperature coefficient of growth suggests that $Fe(C_5H_5)_2$ enhances VA-CNT growth through a surface specific intermediate reaction step that provides active Fe to the predeposited metal catalyst film.

The authors gratefully acknowledge technical assistance by Pamela Fleming. The authors thank M. Guillorn, C.M. Rouleau, and M. Hale for assistance with the photolithographic fabrication of the Center for Nanophase Materials Sciences (CNMS) logo samples. This research was sponsored by the Oak Ridge National Laboratory, managed by UT-Battelle, LLC, for the U.S. Department of Energy under Contract No. DE-AC05-00OR22725 and the Laboratory-Directed Research and Development Program at ORNL.

[1] *Carbon Nanotubes: Synthesis, Structure, Properties, and Applications*, Topics in Applied Physics, Vol. 80, edited by M. S. Dresselhaus, G. Dresselhaus, and Ph. Avouris (Springer, Hiedelberg, 2001).
[2] Z. W. Pan, S. S. Xie, B. H. Chang, C. Y. Wang, L. Lu, W. Liu, W. Y. Zhou, W. Z. Li, and L. X. Qian, Nature (London) **394**, 632 (1998).
[3] H. Dai, Surf. Sci. **500**, 218 (2002).
[4] Z. F. Ren, Z. P. Huang, J. W. Xu, J. H. Wang, P. Bush, M. P. Siegal, and P. N. Provincio, Science **282**, 1105 (1998).
[5] V. I. Merkulov, D. H. Lowndes, Y. Y. Wei, G. Eres, and E. Voelkl, Appl. Phys. Lett. **76**, 3555 (2000).
[6] J. Kong, H. T. Soh, A. M. Cassell, C. F. Quate, and H. Dai, Nature (London) **395**, 878 (1998).
[7] Y. Y. Wei and G. Eres, Appl. Phys. Lett. **76**, 3759 (2000).
[8] Y. Y. Wei and G. Eres, Appl. Phys. Lett. **78**, 1394 (2001).
[9] H. T. Ng, B. Chen, J. E. Koehne, A. M. Cassell, J. Li, J. Han, and M. Meyyappan, J. Phys. Chem. B **107**, 8484 (2003).
[10] L. Delzeit, C. V. Nguyen, B. Chen, R. Stevens, A. Cassell, J. Han, and M. Meyyappan, J. Phys. Chem. B **106**, 5629 (2002).
[11] R. T. K. Baker and P. S. Harris, *Chemistry and Physics of Carbon*, edited by P. L. Walker and P. A. Thrower (Marcel Dekker, New York, 1978), Vol 14, pp. 83–165.
[12] P. E. Nolan, D. C. Lynch, and A. H. Cutler, J. Phys. Chem. B **102**, 4165 (1998).
[13] D. B. Geohegan, A. A. Puretzky, I. N. Ivanov, S. Jesse, G. Eres, and J. Y. Howe, Appl. Phys. Lett. **83**, 1851 (2003).
[14] H. Cui, G. Eres, J. Y. Howe, A. Puretzky, M. Varela, D. B. Geohegan, and D. H. Lowndes, Chem. Phys. Lett. **374**, 222 (2003).
[15] B. C. Satishkumar, A. Govindaraj, and C. N. R. Rao, Chem. Phys. Lett. **307**, 158 (1999).
[16] C. Singh, M. S. P. Shaffer, and A. Windle, Carbon **41**, 359 (2003).
[17] H. Hou, A. K. Schaper, F. Weller, and A. Greiner, Chem. Mater. **14**, 3990 (2002).
[18] A. Cao, X. Zhang, C. Xu, J. Liang, D. Wu, X. Chen, B. Wei, and P. M. Ajayan, Appl. Phys. Lett. **79**, 1252 (2001).
[19] G. J. M. Dormans, J. Cryst. Growth **108**, 806 (1991).
[20] K. E. Lewis and G. P. Smith, J. Am. Chem. Soc. **106**, 4650 (1984).
[21] T. de los Arcos, F. Vonau, M. G. Garnier, V. Thommen, H.-G. Boyen, P. Oelhafe, M. Duggelin, D. Mathis, and R. Guggenheim, Appl. Phys. Lett. **80**, 2383 (2002).
[22] L. S. Lobo and D. L. Trimm, Nature (London) Phys. Sci. **234**, 15 (1971).